Electronic Supplementary Material (ESI) for Dalton Transactions.

μ–Pyridine bridged Copper Complex with Robust Proton Reducing Ability

Karunamay Majee, Jully Patel, Babulal Das, and Sumanta Kumar Padhi

Supporting Information

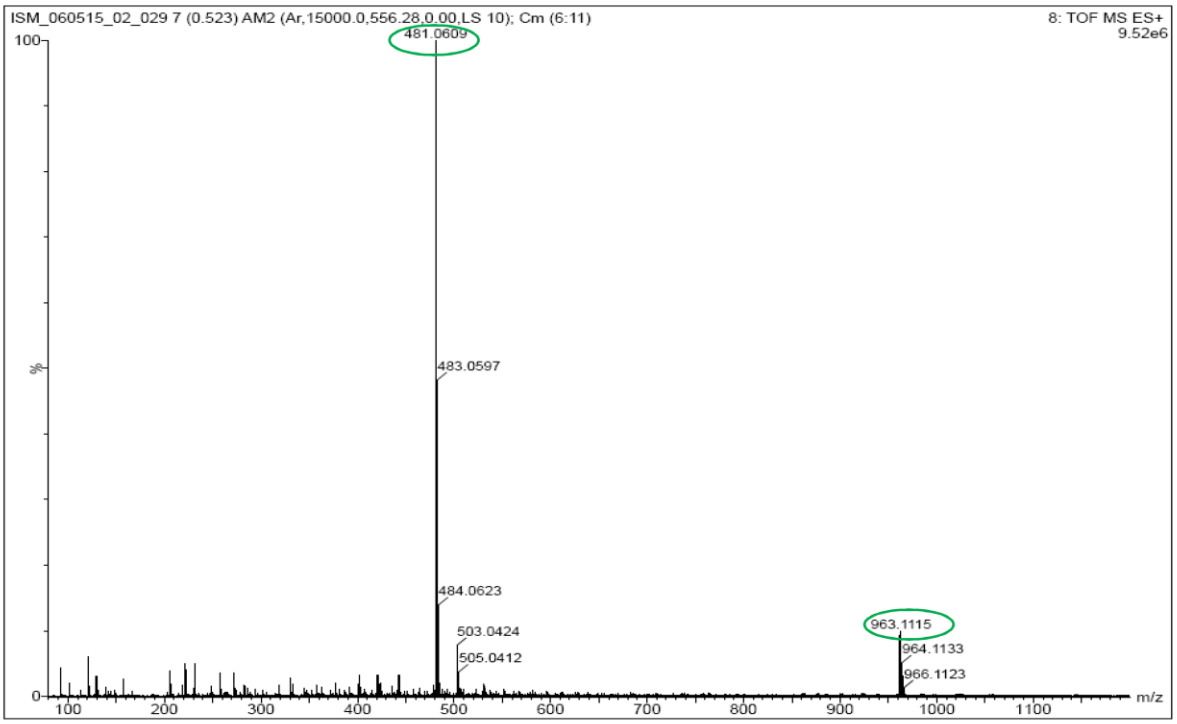

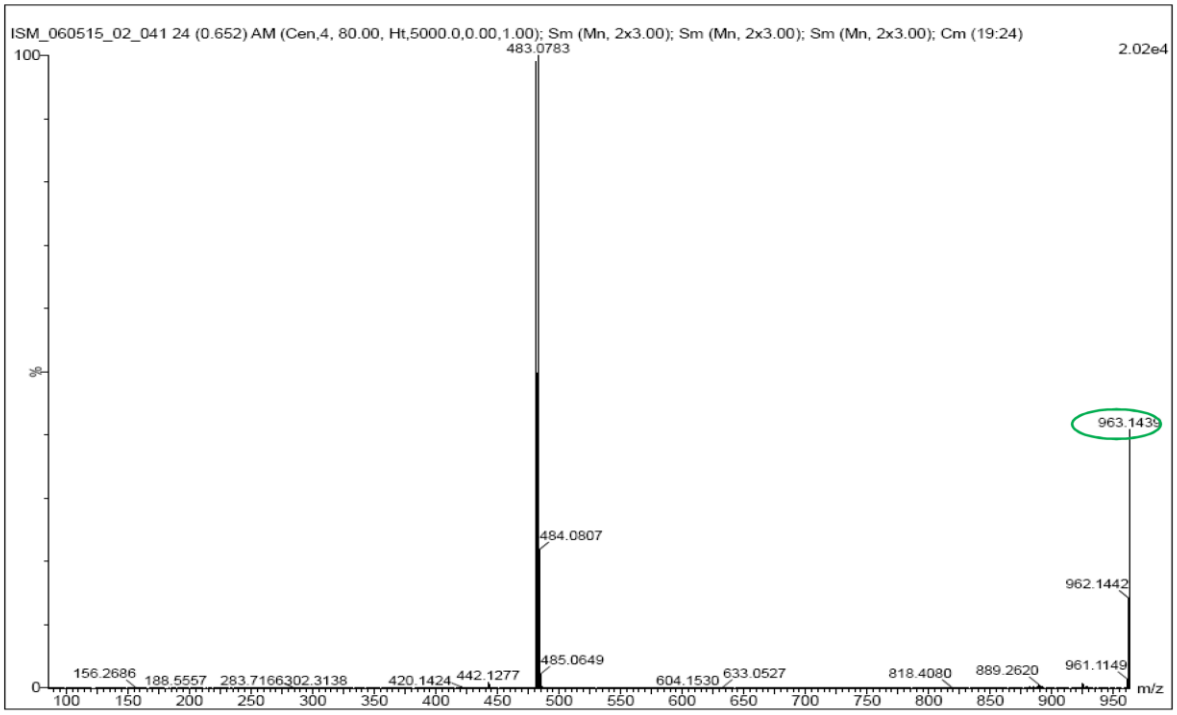

Figure S0: Mass spectra of $[Cu(DQPD)]_2$ in DMF (Top; MS Spectra in centroid Mode and bottom: MSMS spectra at 963.1115).

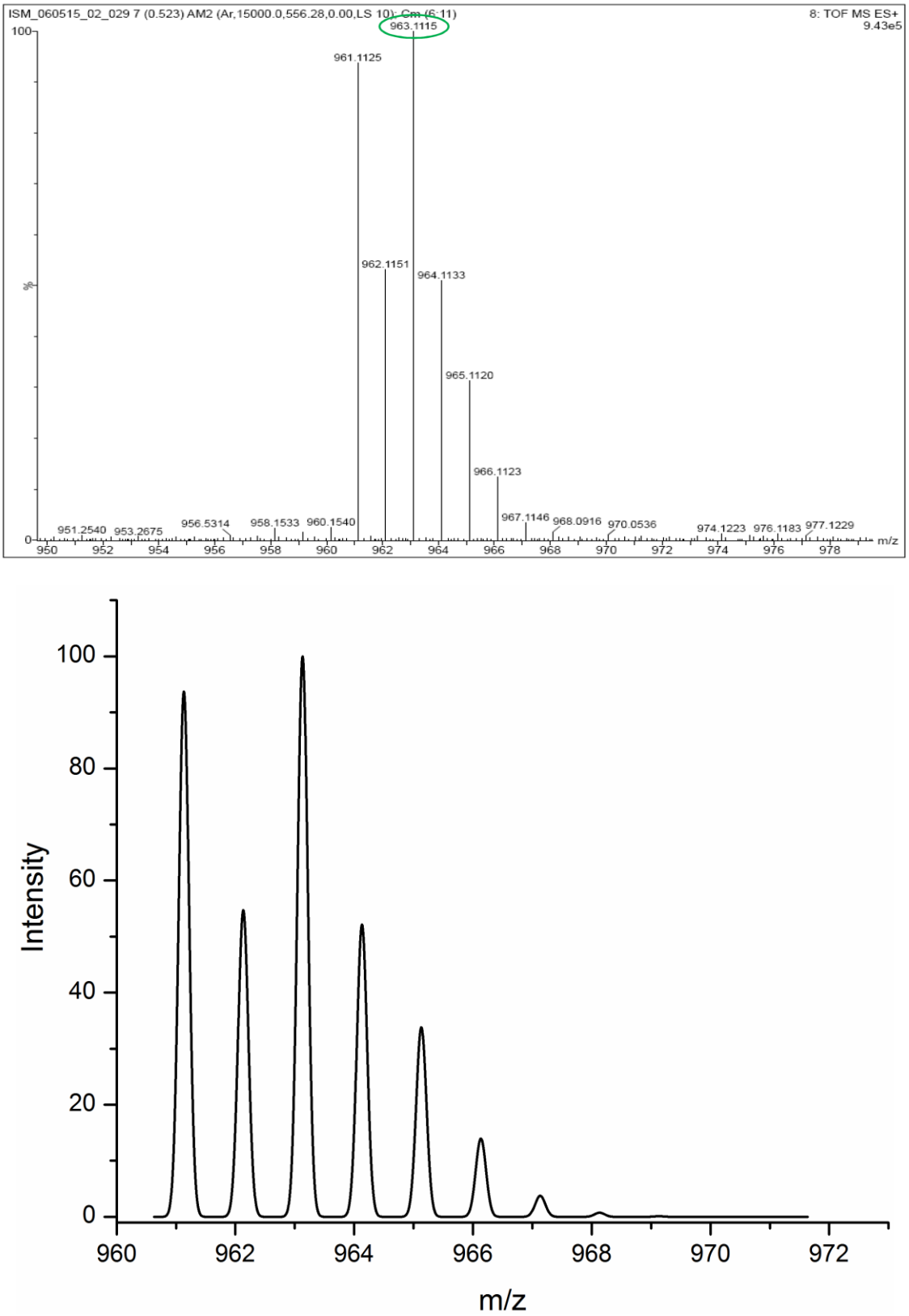

Figure S1: Mass spectra of $[Cu(DQPD)]_2$ in DMF (Top; Experimental and Bottom: Simulated).

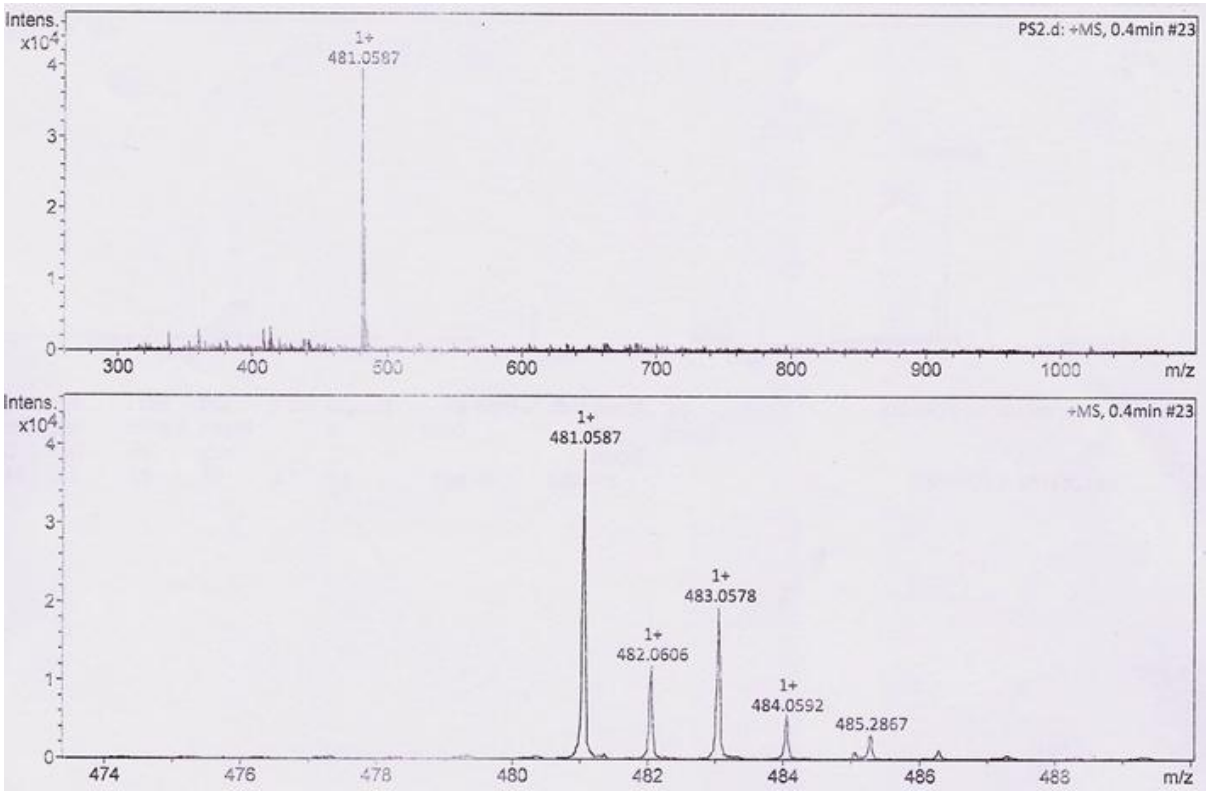

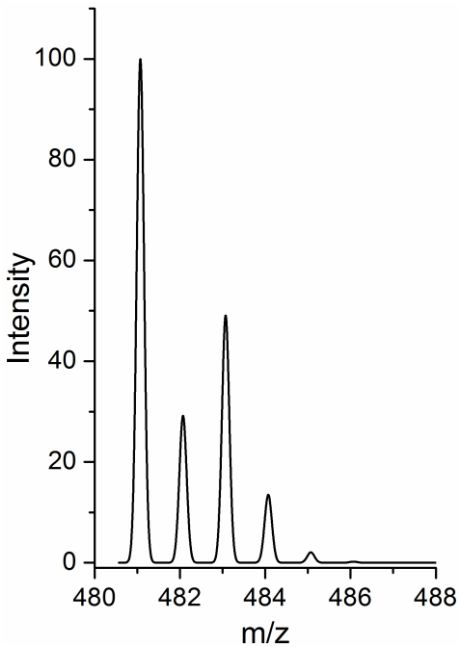

Figure S2: Mass spectra of $[Cu(DQPDH)]^+$ in DMF (Top; Experimental and bottom: simulated).

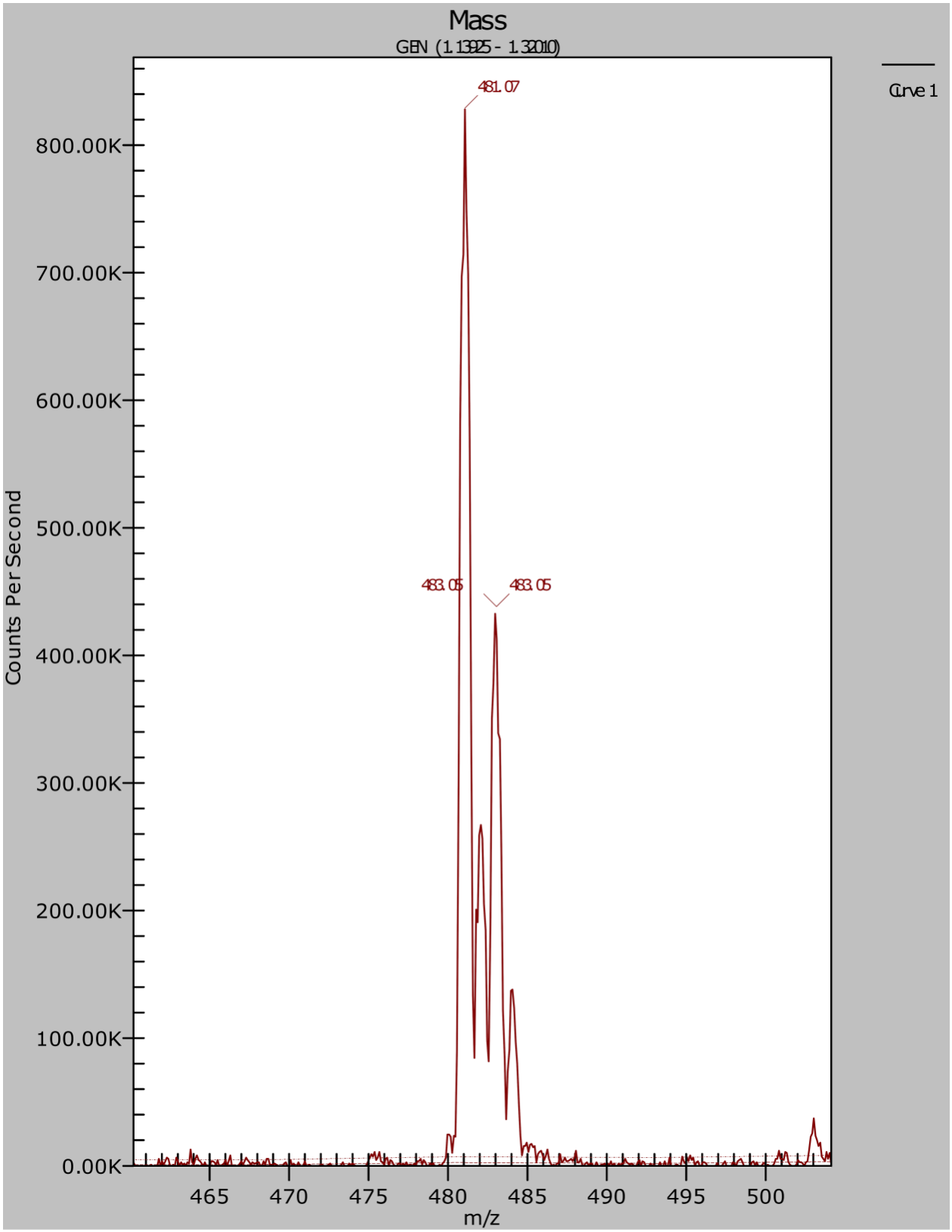

Figure S3: Mass spectra of *in situ* formed $[Cu(DQPDH)]^+$ in DMF/H_2O 95:5 v/v.

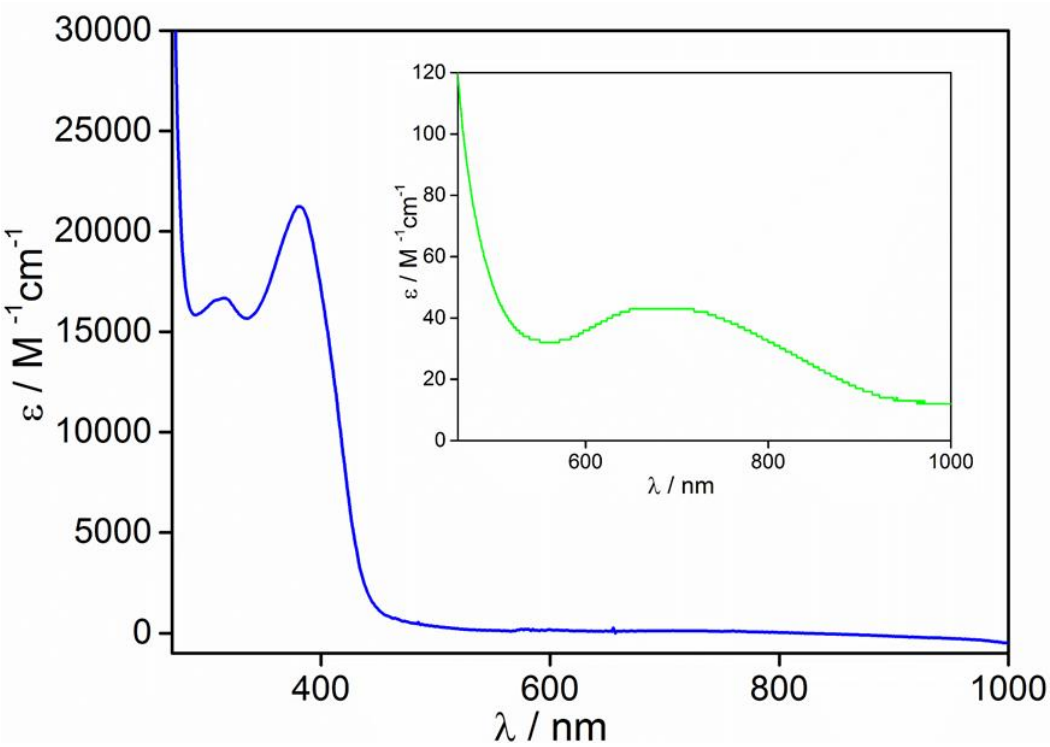

Figure S4: UV-Vis spectra of 0.05 mM $[Cu(DQPD)]_2$ in DMF. Inset shows the d-d transition of the complex (1mM).

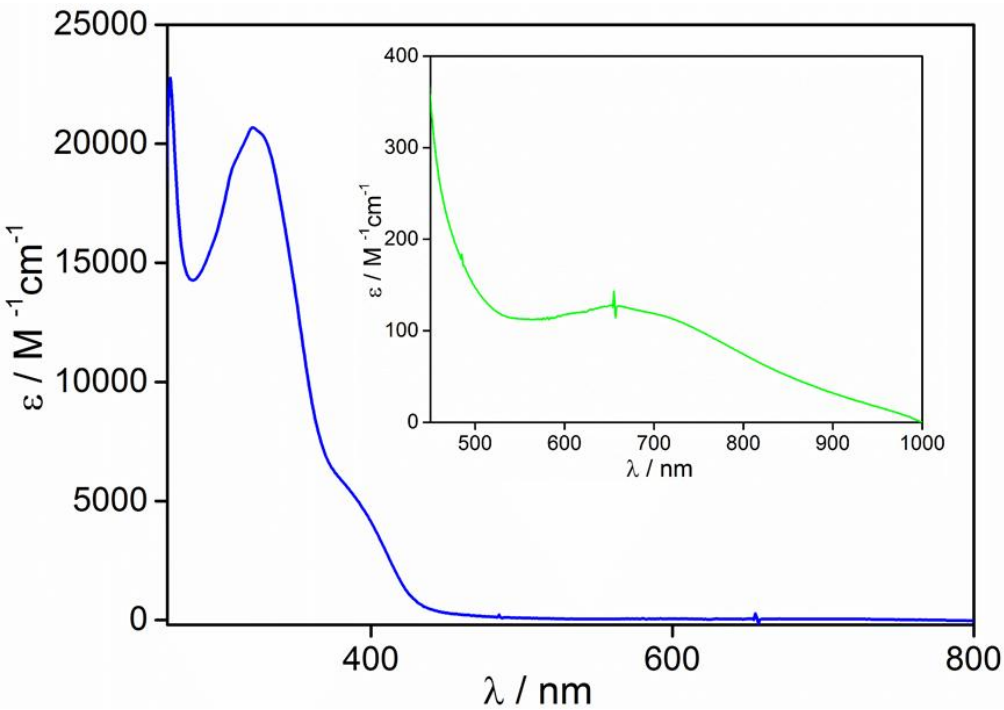

Figure S5: UV-Vis spectra of 0.05 mM $[Cu(DQPDH)]^+$ in DMF. Inset shows the d-d transition of the complex (1mM).

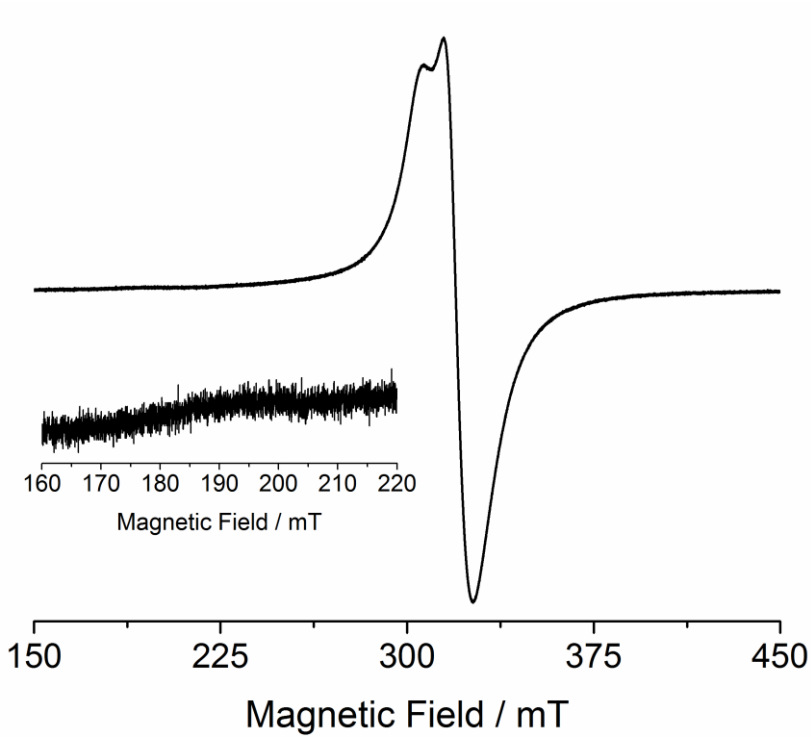

Figure S6: EPR spectra of $[Cu(DQPD)]_2$ complex in DMF.

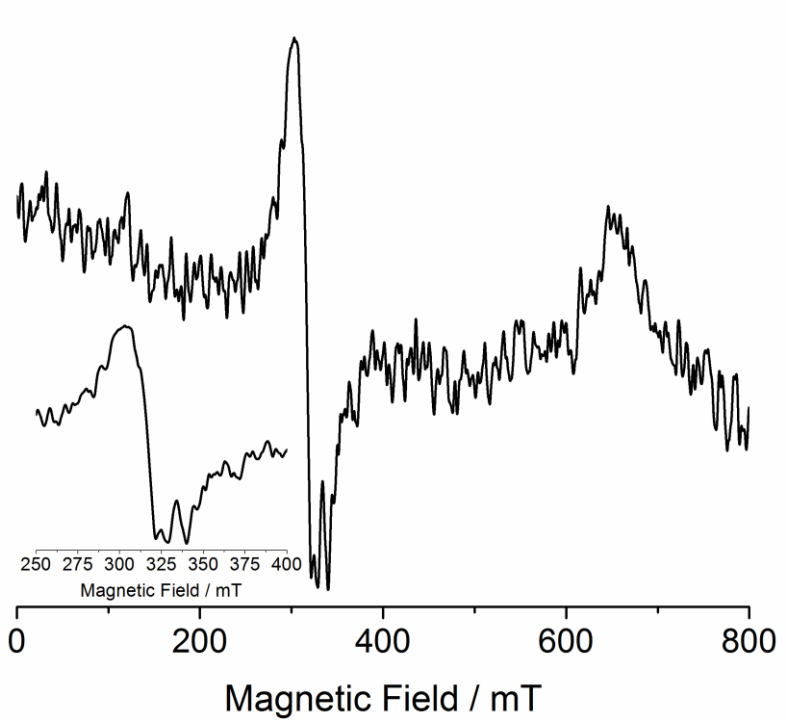

Figure S7: EPR spectra of solid $[Cu(DQPD)]_2$ complex.

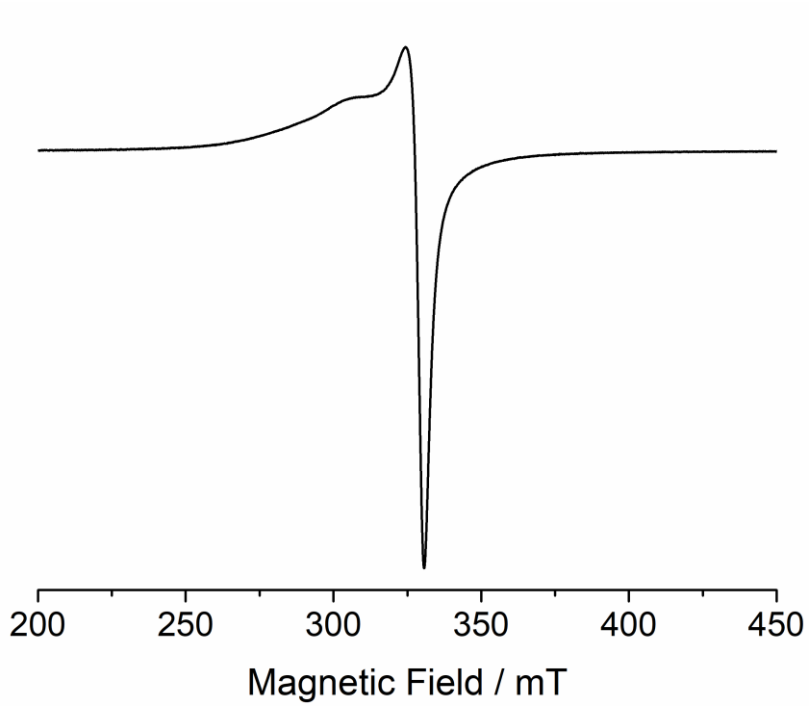

Figure S8: EPR spectra of mononuclear $[Cu(DQPDH)]^+$ complex.

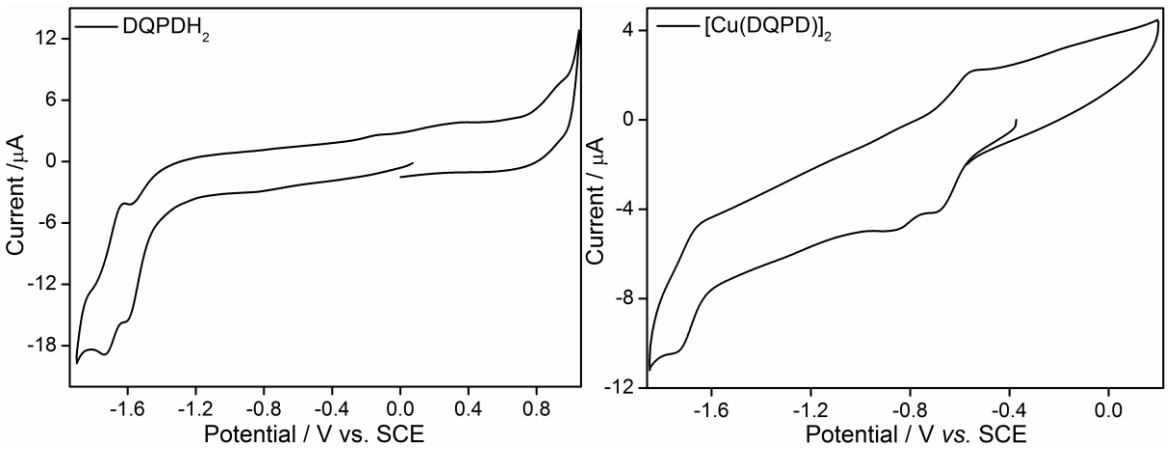

Figure S9: (Left) The Cyclic Voltammogram of the ligand $DQPDH_2$ (1.0 mM) in DMF, 0.1 M TBAP, and an electrochemical potential scan rate of 100 mV s^{-1}. **(Right)** The Cyclic Voltammogram of 1.0 mM $[Cu(DQPD)]_2$ complex in DMF containing 0.1 M TBAP as supporting electrolyte and a scan rate of 100 mV s^{-1} under N_2 atmosphere (The resting potential is at -0.375 V vs. SCE).

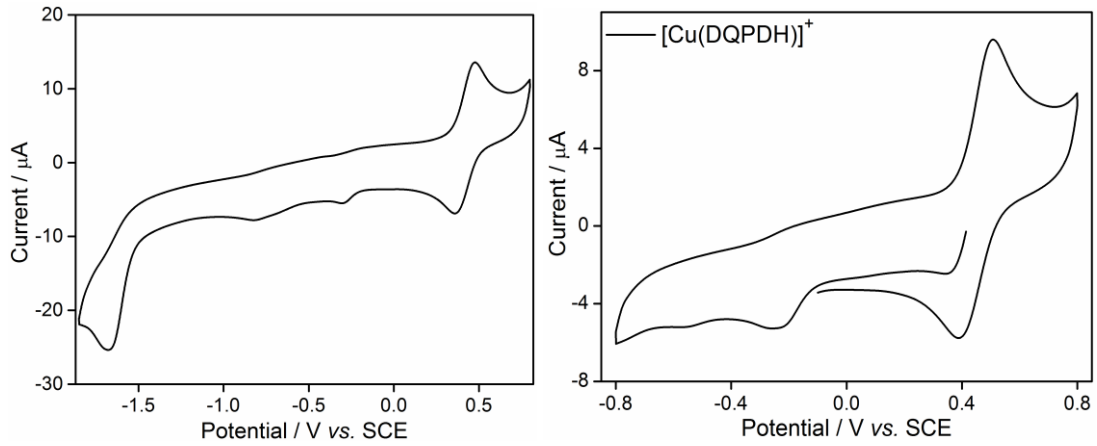

Figure S10: (**Left**) CV of 1.0 mM $[Cu(DQPDH)]^+$ in DMF containing 0.1 M TBAP as supporting electrolyte and a scan rate of 100 mV s^{-1} under N_2 atmosphere; (**Right**) The resting potential is at +0.414 V vs. SCE.

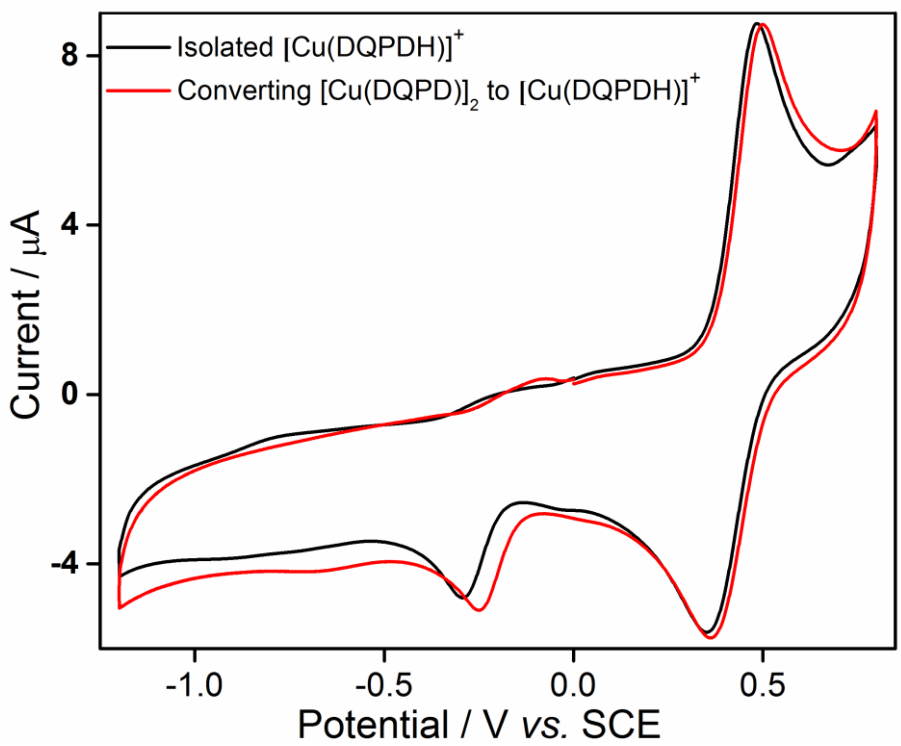

Figure S11: Cyclic Voltammogram of *in situ* generated $[Cu(DQPDH)]^+$ from $[Cu(DQPD)]_2$ by addition of 2 equiv. pTsOH (red) and isolated $[Cu(DQPDH)]^+$ (black) in DMF/H_2O (95:5, v/v) containing 0.1 M TBAP as supporting electrolyte and a scan rate of 100 mV s^{-1} under N_2 atmosphere.

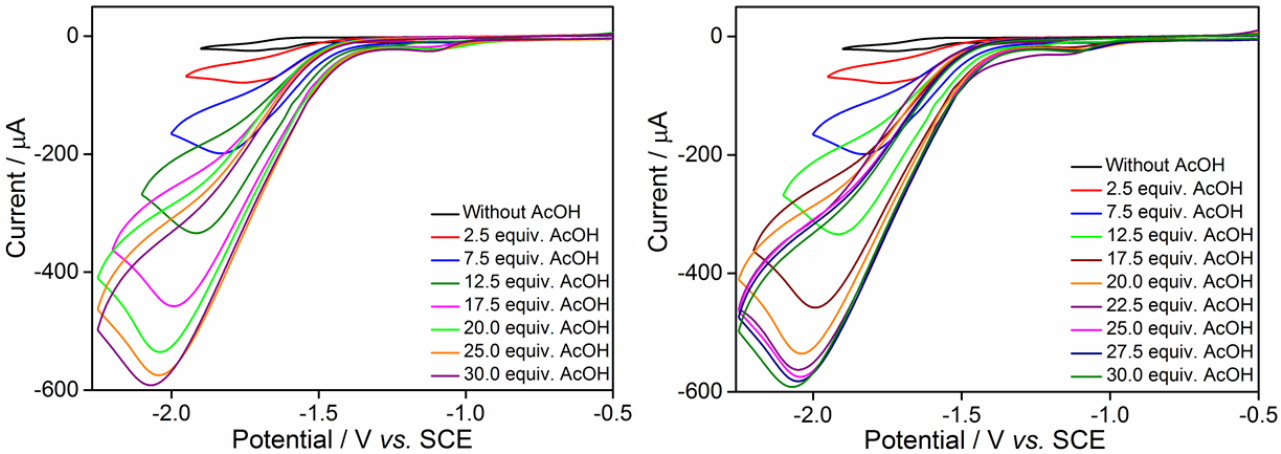

Figure S12: Cyclic voltammogram of 1 mM $[Cu(DQPDH)]^+$ complex with varying concentration of acetic acid in DMF/H_2O (95:5 , v/v) containing 0.1 M TBAP and a scan rate of 100 mV s^{-1} under N_2 atmosphere (left). CV of the complex with varying concentration of acetic acid in DMF/H_2O (95:5 , v/v) showing saturation of catalytic current after addition of 25 equivalent of acetic acid (right).

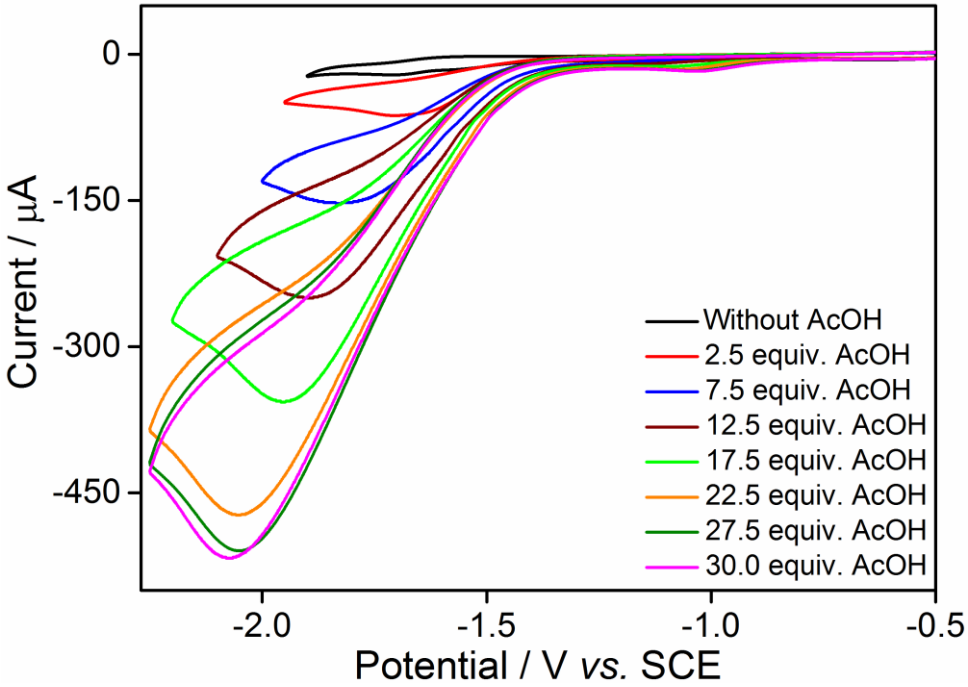

Figure S13: : Cyclic voltammogram of 0.5 mM $[Cu(DQPDH)]^+$ complex with varying concentration of acetic acid in DMF/H_2O (95:5 , v/v) containing 0.1 M TBAP and an electrochemical potential scan rate of 100 mV s^{-1} under N_2 atmosphere.

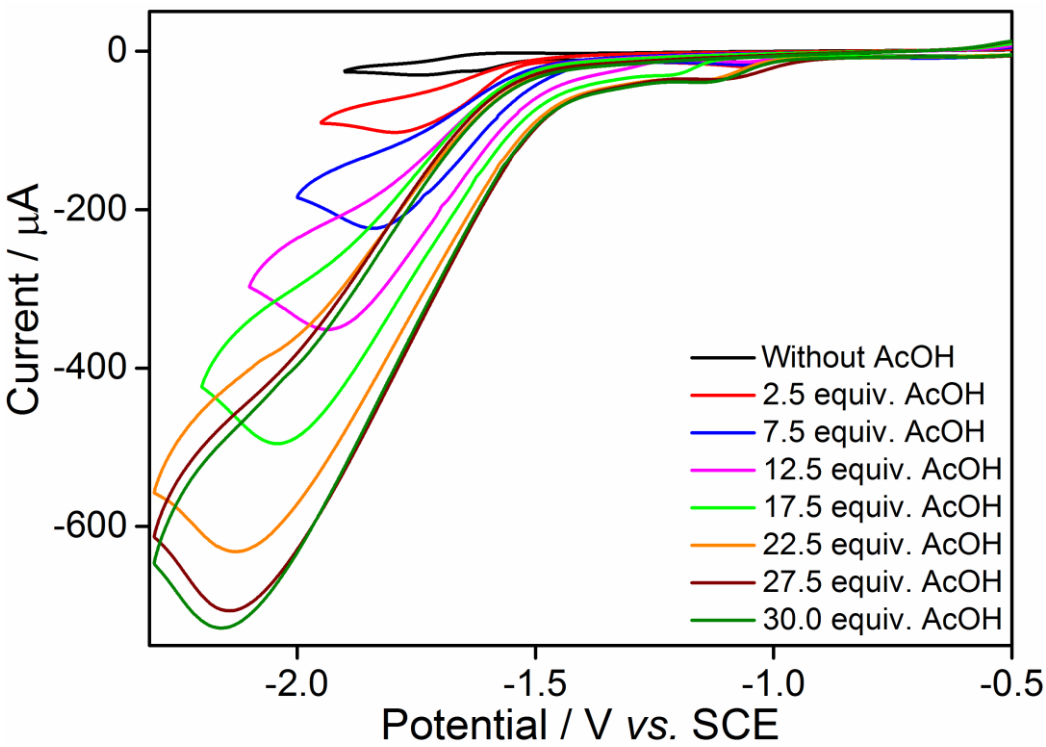

Figure S14: Cyclic voltammogram of 1.5 mM $[Cu(DQPDH)]^+$ complex with varying concentration of acetic acid in DMF/H_2O (95:5 , v/v) containing 0.1 M TBAP and an electrochemical potential scan rate of 100 mV s^{-1} under N_2 atmosphere.

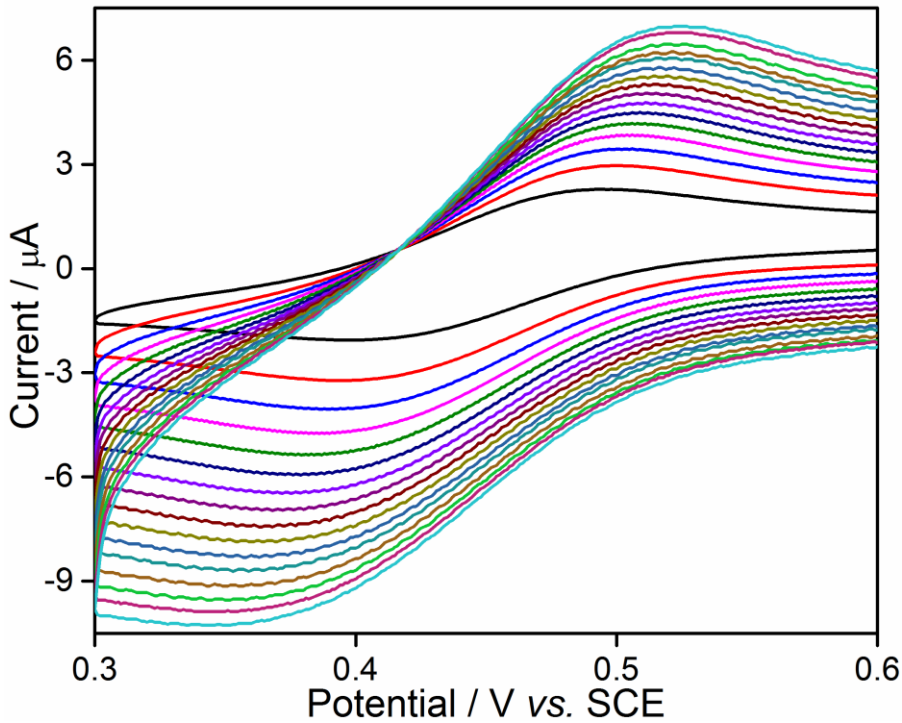

Figure S15: Cyclic voltammogram of 1 mM $[Cu(DQPDH)]^+$ complex in presence of 0.1 M TBAP as supporting electrolyte in DMF/H_2O (95:5, v/v) solution at varying scan rates (25 mV s^{-1} to 400 mV s^{-1}).

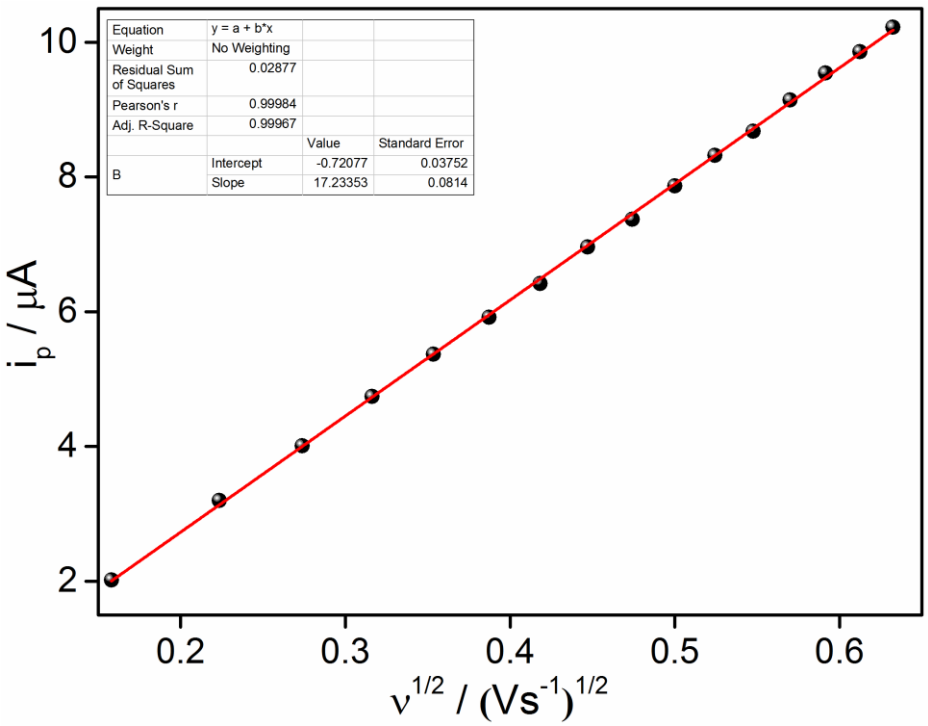

Figure S16: Peak current (i_p) vs. square root of scan rate ($v^{1/2}$) with linear fitted slop 1.7 x 10^{-5} $AV^{-1/2}$ $s^{-1/2}$.

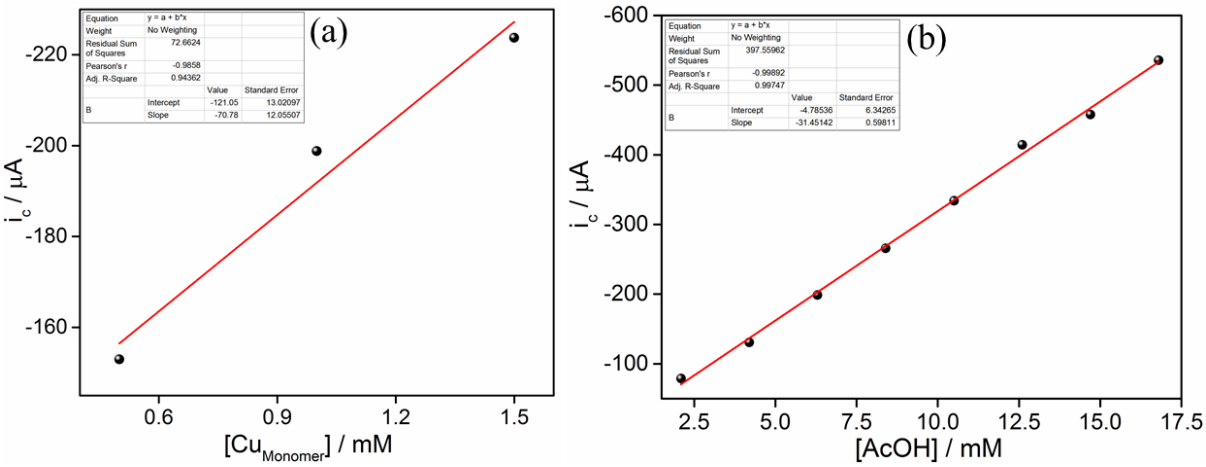

Figure S17: Dependence of catalytic current, i_c, (a) on complex concentration in presence of 7.5 equivalent of acetic acid. (b) On acetic acid concentration for a catalyst concentration of 1.0 mM at a scan rate of 100 mV s^{-1}.

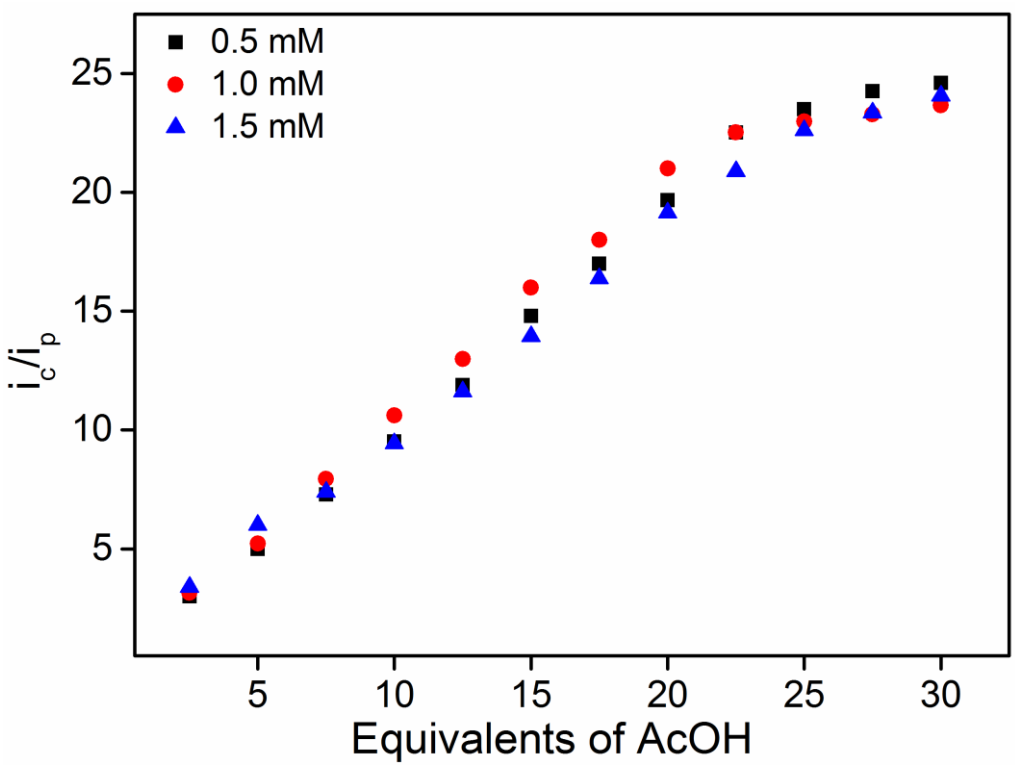

Figure S18: Dependence of i_c/i_p, on acetic acid concentration for three different catalyst concentrations of 0.5, 1.0 and 1.5 mM in presence of 0.1 M TBAP as supporting electrolyte in DMF/H_2O (95:5, v/v) at potential scan rate of 100 mV s^{-1}.

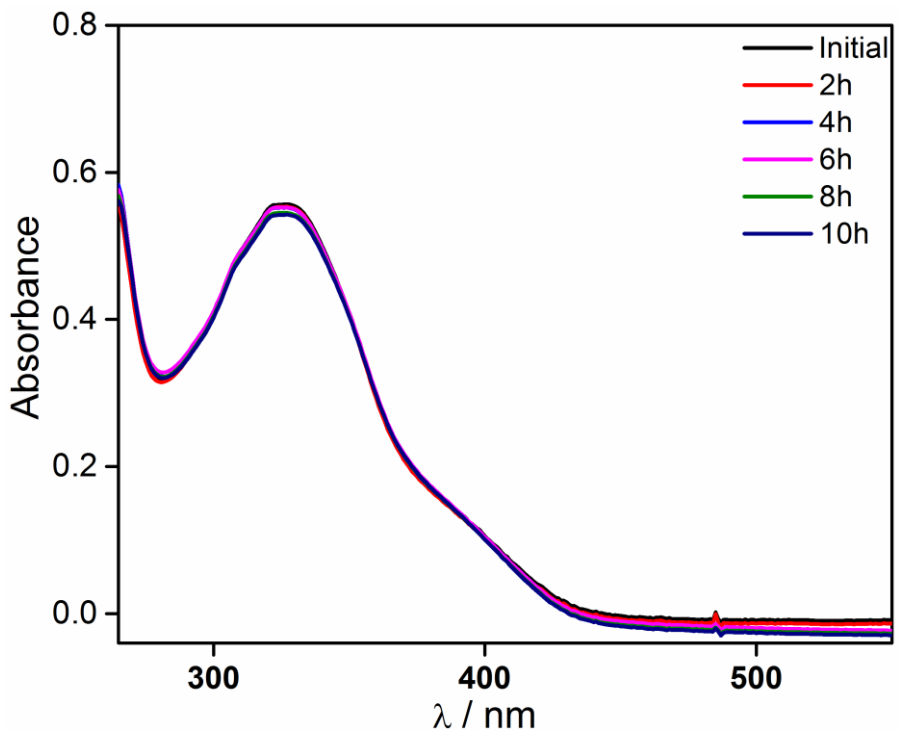

Figure S19: The UV-Visible spectrum of 0.05 mM $[Cu(DQPDH)]^+$ complex in presence of 25 equivalent acetic acid in DMF/H_2O (95:5 , v/v) upto 10 hours.

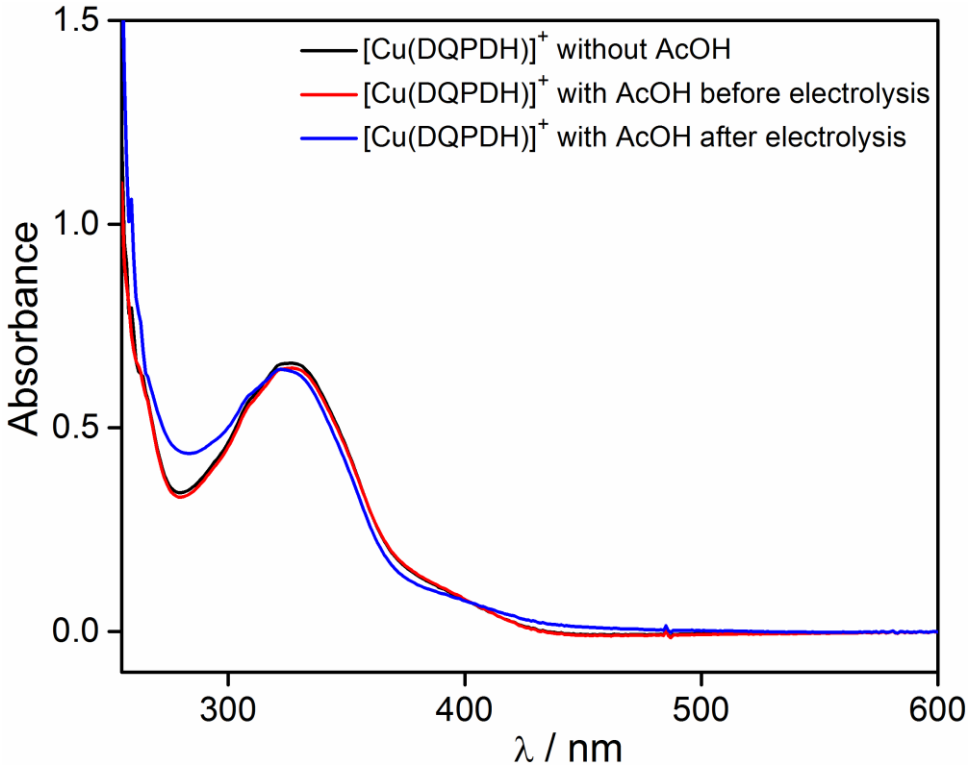

Figure S20: UV -Visible spectra of 0.05 mM complex before and after bulk electrolysis on adding 25 equivalent of acetic acid at potential -1.6 V vs. SCE under inert atmosphere.

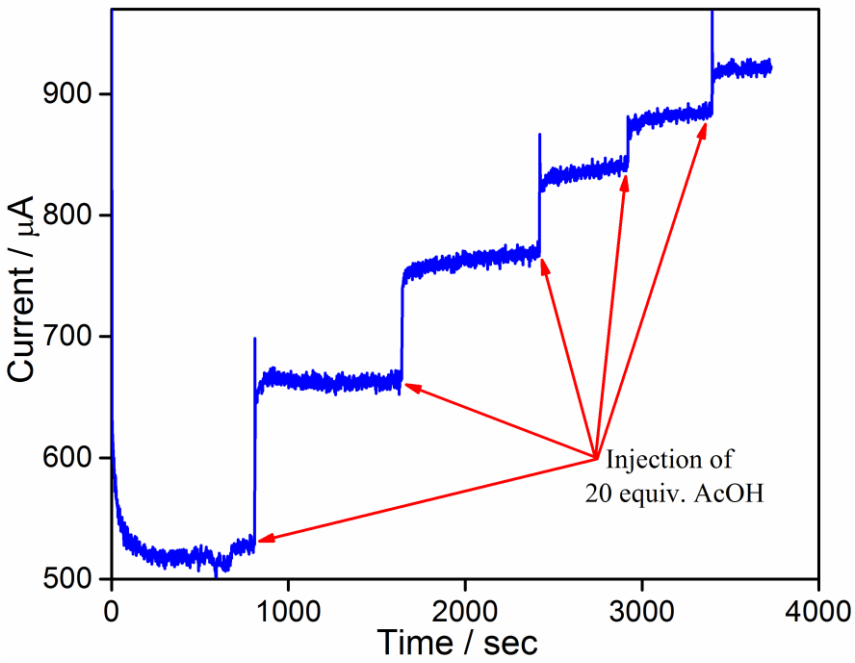

Figure S21: Current curve of 0.05mM $[Cu(DQPDH)]^+$ during electrolysis at -1.6 V vs. SCE in DMF/H_2O (95:5 , v/v) using 0.1M TBAP as supporting electrolyte.

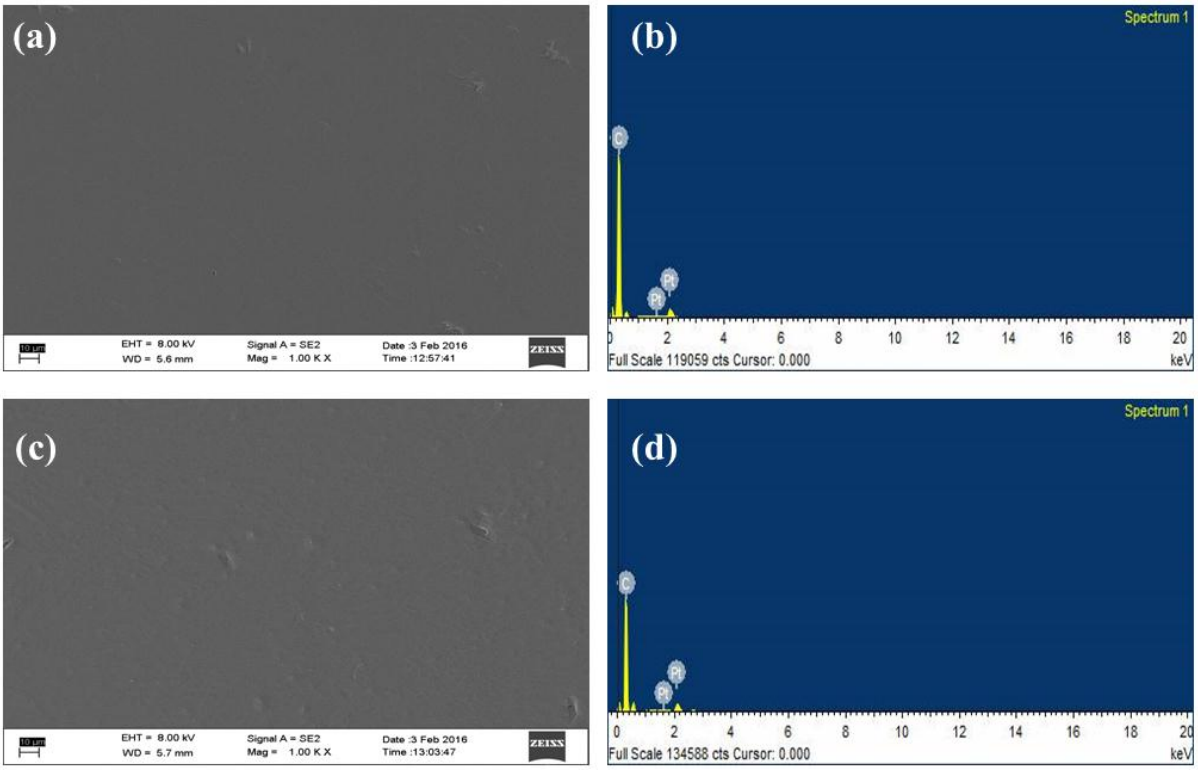

Figure S22: FESEM image of glassy carbon plate (a) before bulk elctrolysis and (c) after bulk electrolysis of 2 hours at -1.6 V vs. SCE. EDX data of glassy carbon plate (b) before bulk electrolysis and (d) after bulk electrolysis of 2 hours at -1.6 V vs. SCE. Electrolysis condition: 0.05 mM $[Cu(DQPDH)]^+$ with 25 equivalent acetic acid in DMF/H_2O (95:5 , v/v) using 0.1 M TBAP as supporting electrolyte.

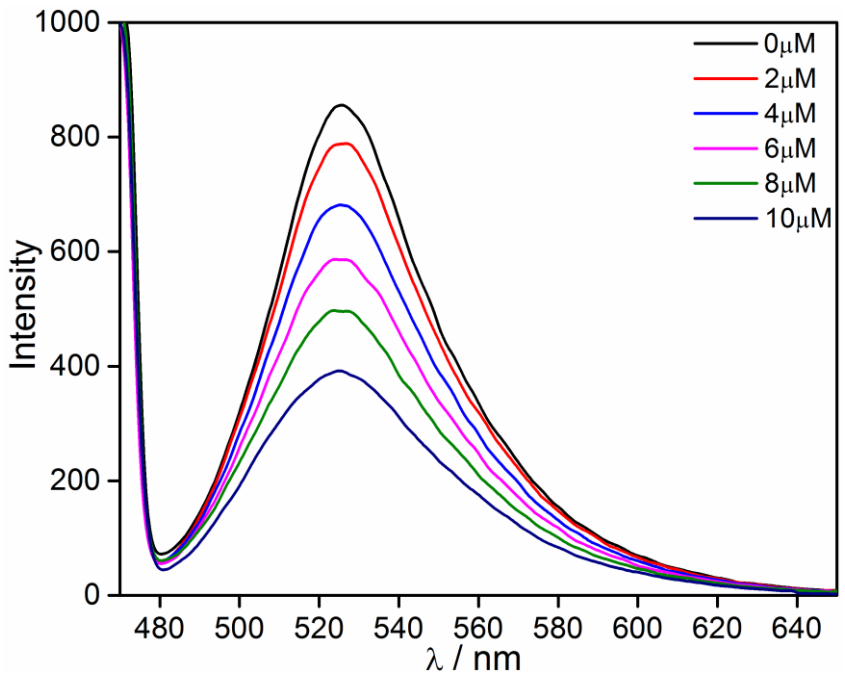

Figure S23: The fluorescence quenching of fluorescein by $[Cu(DQPD)]_2$ in DMF/H_2O (80:20, v/v).

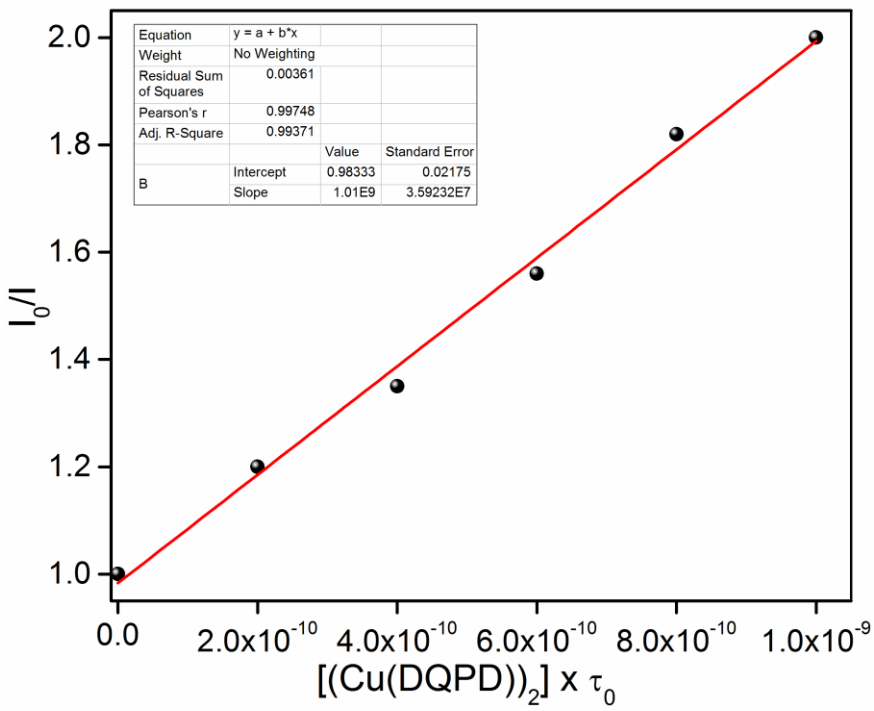

Figure S24: Stern-Volmer plot of emission quenching of 5×10^{-8} M fluorescein solution by $[Cu(DQPD)]_2$ in DMF/H_2O (80:20, v/v).

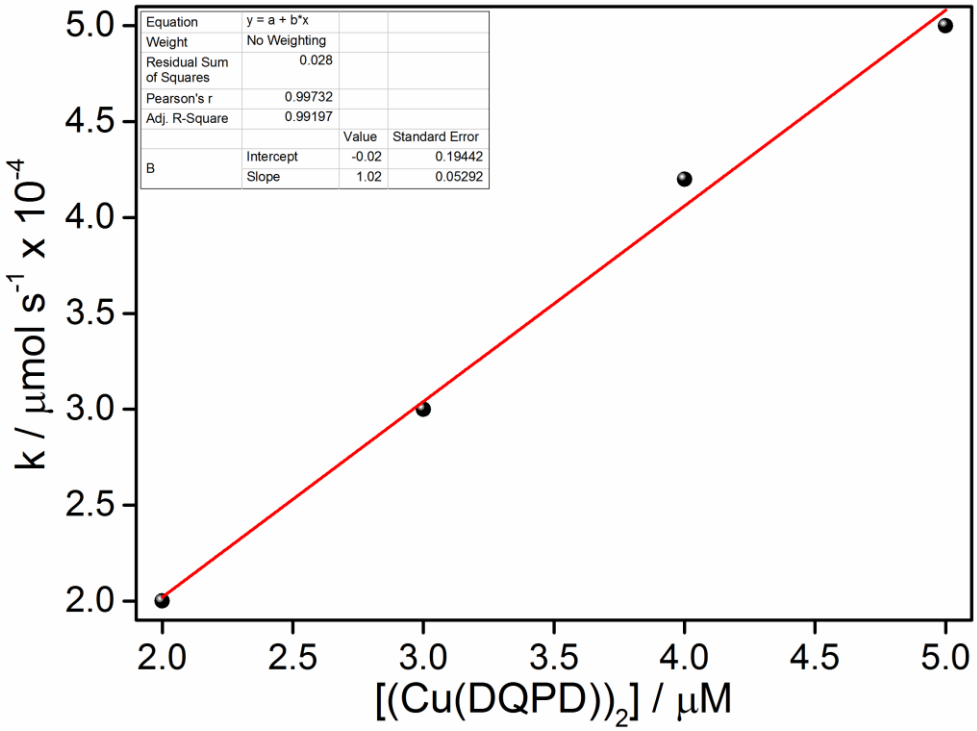

Figure S25: Rate of hydrogen production with varied concentration of $[Cu(DQPD)]_2$ in presence of 2mM fluorescein and 0.36 M TEA in 80:20 (v/v) DMF/H_2O.

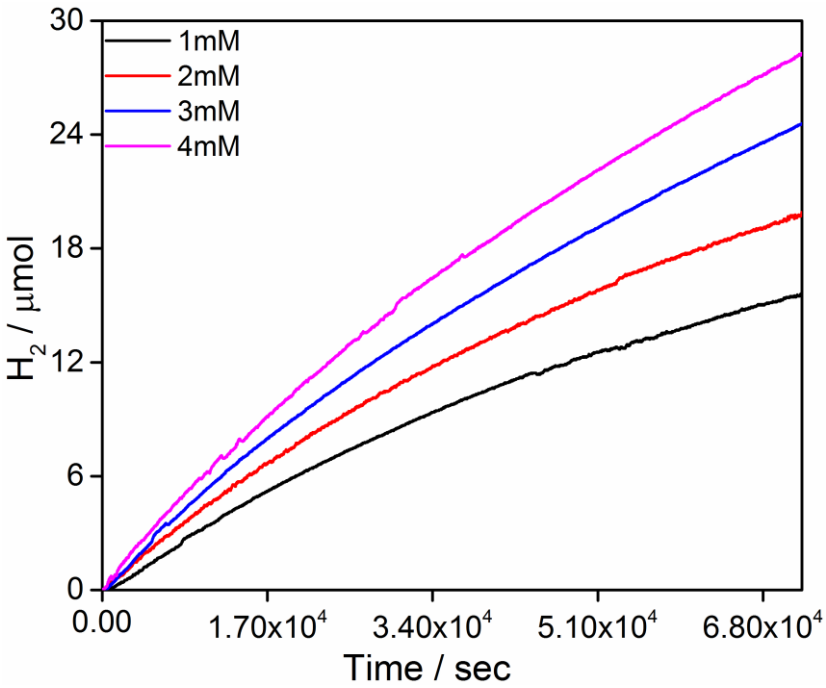

Figure S26: Hydrogen production with $[Cu(DQPD)]_2$ = 4.0 × 10^{-6} M and [TEA] = 0.36 M in DMF/H_2O (80: 20, v/v) with various [Fl] from 1– 4 mM.

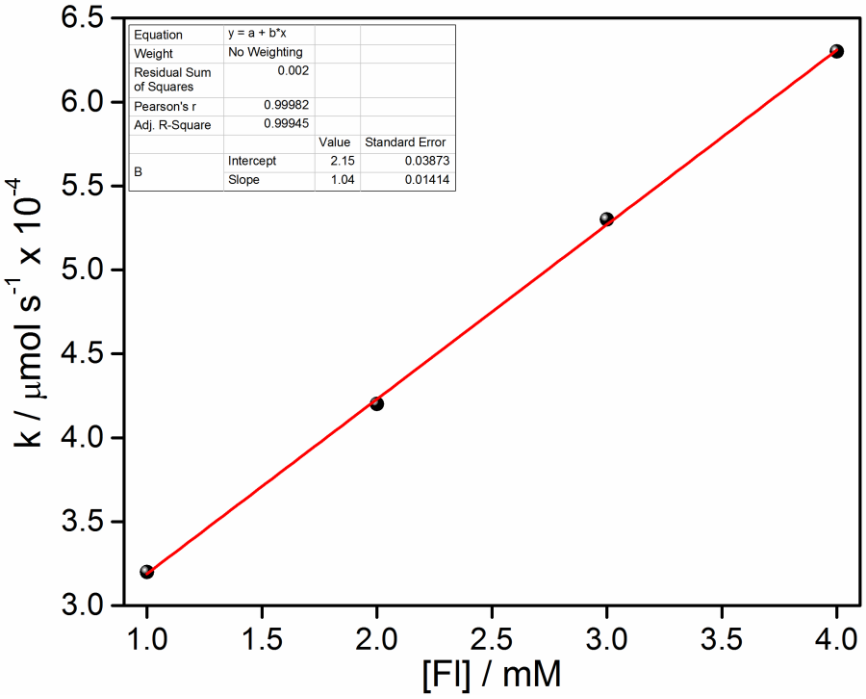

Figure S27: Rate of hydrogen production with varied concentration of [Fl] in presence of 4.0 × 10^{-6} M $[Cu(DQPD)]_2$ and 0.36 M TEA in 80:20 (v/v) DMF/H_2O.

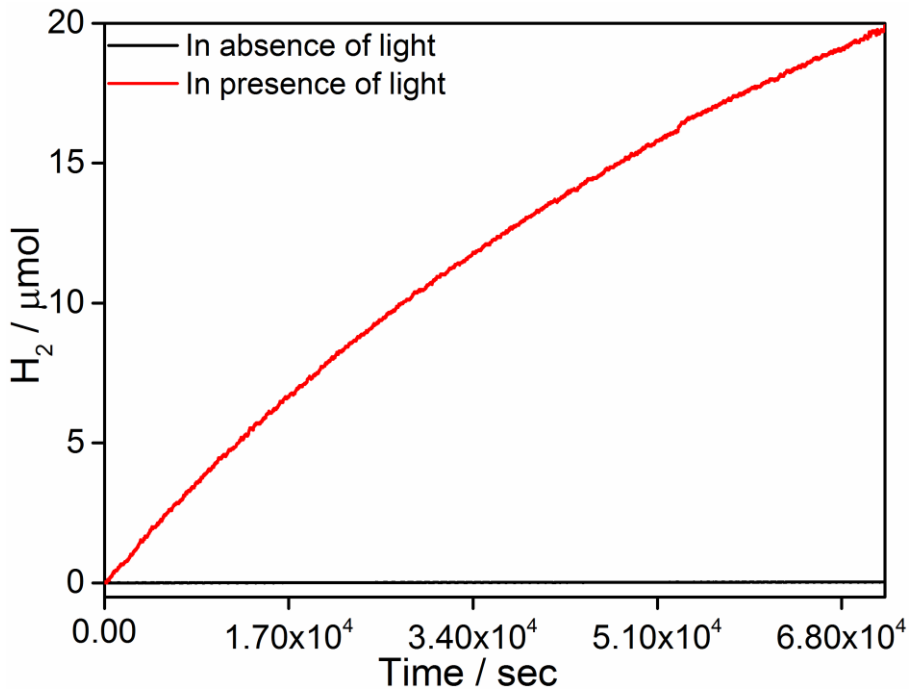

Figure S28: Hydrogen production with 4.0 × 10^{-6} M $[Cu(DQPD)]_2$ in presence of 2 mM fluorescein and 0.36 M TEA in 80:20 (v/v) DMF/H_2O in presence of light (red) and under dark condition (black).

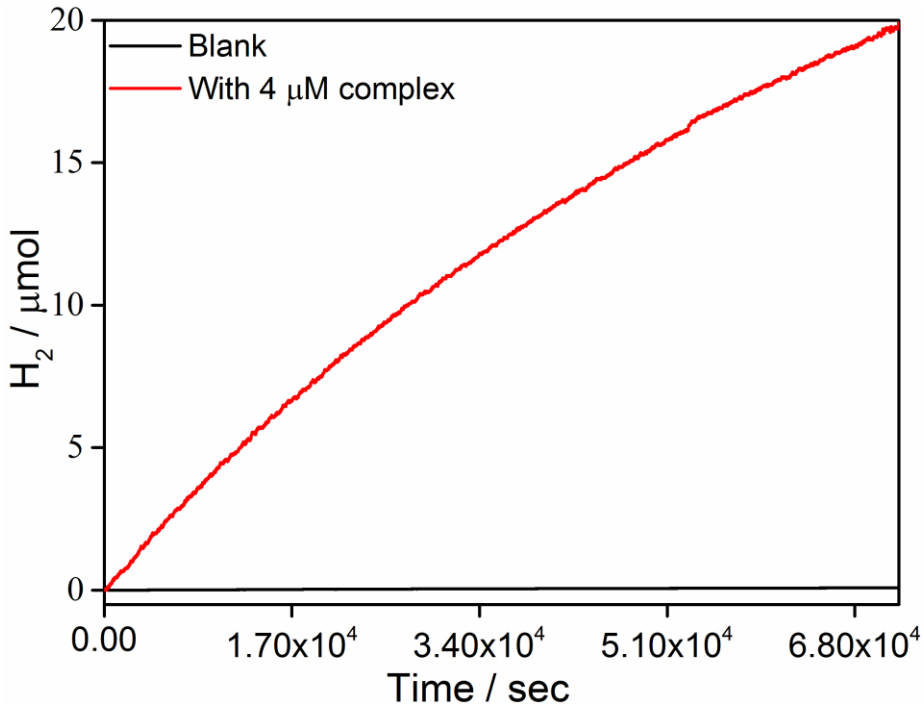

Figure S29: Hydrogen evolution by 4.0 × 10^{-6} M $[Cu(DQPD)]_2$ in presence of 2 mM fluorescein and 0.36 M TEA in 80:20 (v/v) DMF/H_2O (red) and blank solution in absence of catalyst (black).

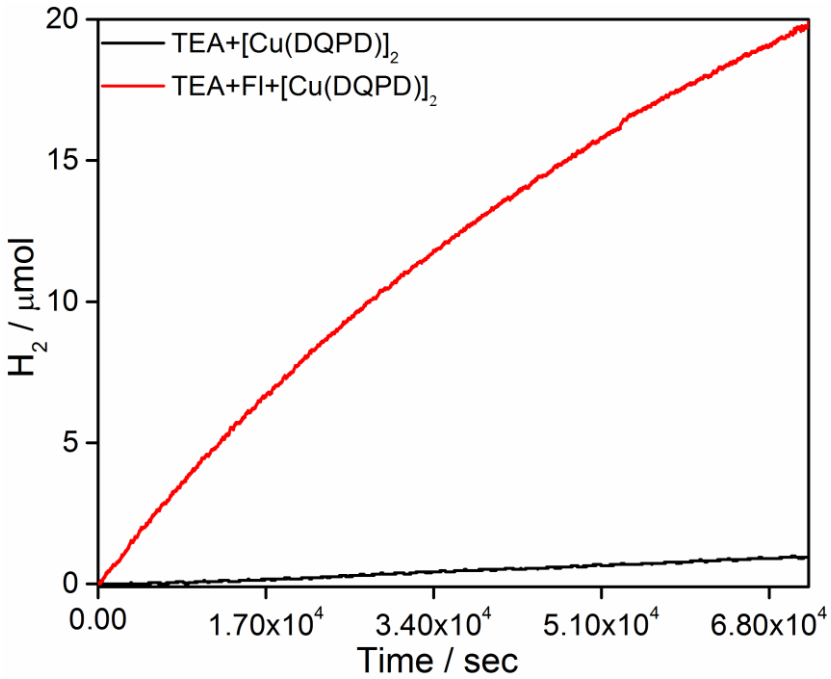

Figure S30: Hydrogen evolution by 4.0×10^{-6} M $[Cu(DQPD)]_2$ in the presence of 0.36 M TEA and 2 mM fluorescein in 80 : 20 (v/v) DMF/H_2O (red) and 4.0×10^{-6} M $[Cu(DQPD)]_2$ in the presence of 0.36 M TEA without fluorescein (black).

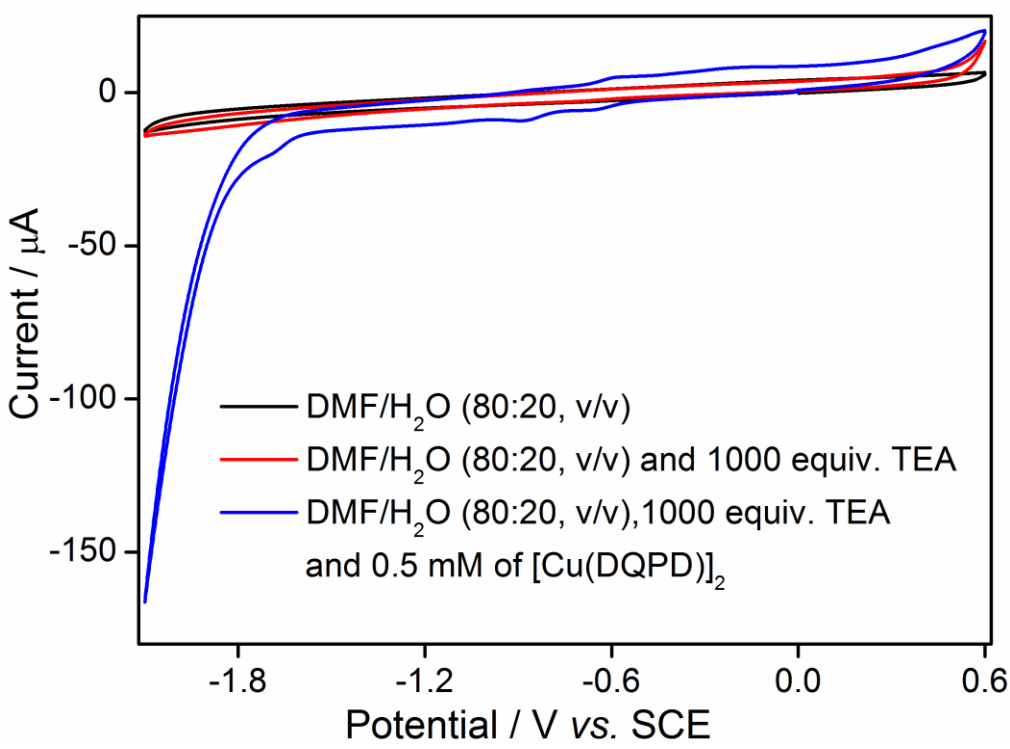

Figure S31: The cyclic voltammogram of blank 80:20 (v/v) DMF/H_2O (black), in presence of 1000 equiv. TEA (red), and upon addition of 0.5 mM $[Cu(DQPD)]_2$ (Blue).

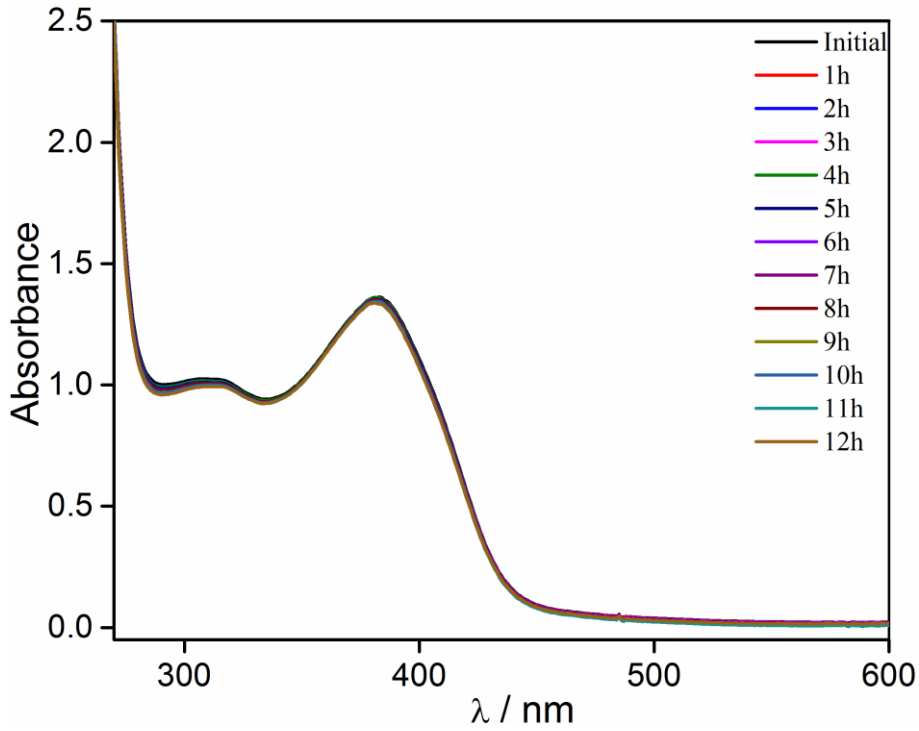

Figure S32: The UV-Visible spectrum of 0.05mM $[Cu(DQPD)]_2$ complex with irradiation of light in DMF/H_2O (80:20 , v/v) upto 12 hours.

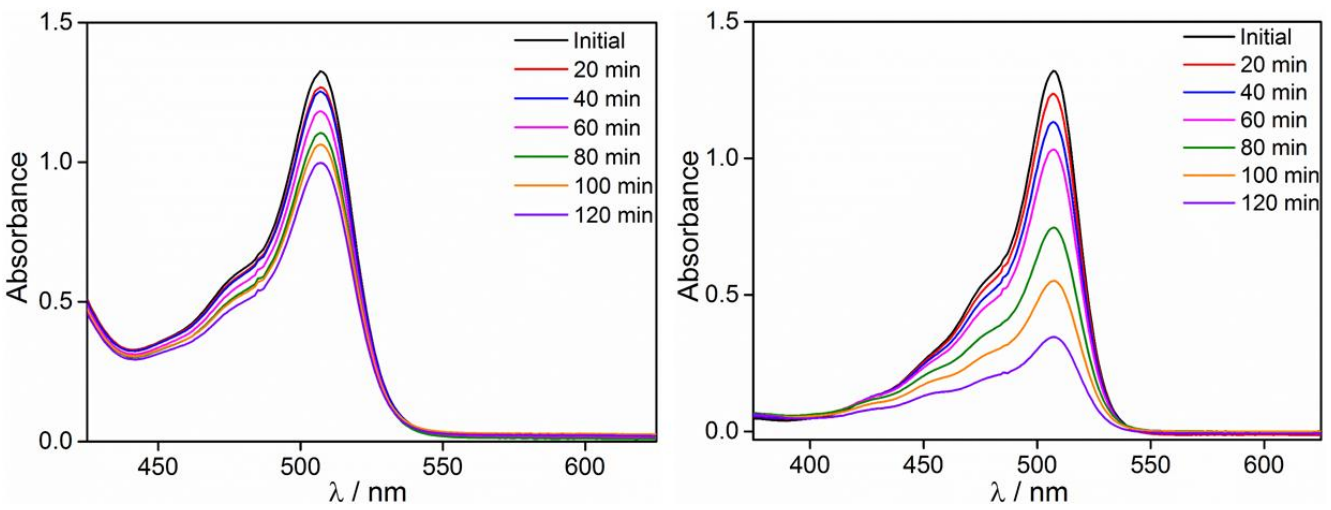

Figure S33: UV-vis spectral change of the system containing fluorescein (4 x 10^{-5} M), $[Cu(DQPD)]_2$ (8 x 10^{-5} M) and TEA (4 x 10^{-5} M) in 80:20 (v/v) DMF/H_2O (left). UV-vis spectral change of the system containing fluorescein (4 x 10^{-5} M) and TEA (4 x 10^{-5} M) in DMF/H_2O (80:20, v/v) (Right).

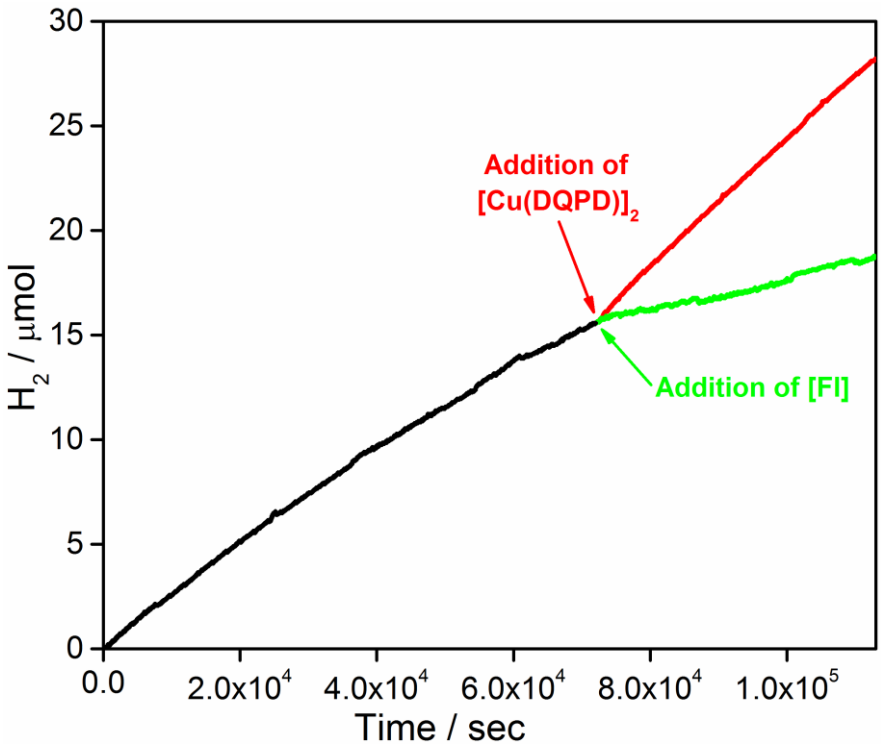

Figure S34 : Hydrogen production by 4.0×10^{-6} M $[Cu(DQPD)]_2$ complex in 80:20 (v/v) DMF/H_2O in presence of 1 mM fluorescein and 0.36 M TEA (black) and the recovery of the photocatalytic activity by the addition of extra Fl (1.0 mM) or 4.0×10^{-6} M $[Cu(DQPD)]_2$ after 22 h irradiation.

Table S1 Crystal data and structure refinement for $[Cu(DQPD)]_2 \cdot DMF \cdot H_2O$

Identification code	**$[Cu(DQPD)]_2$**
CCDC Number	1564520
Empirical formula	$C_{53}H_{39}Cu_2N_{11}O_6$
Formula weight	1053.05
Temperature/K	296.15
Crystal system	monoclinic
Space group	$P2_1/n$
a/Å	11.3335(5)
b/Å	28.1780(10)
c/Å	15.8677(6)
α/°	90
β/°	109.306(2)
γ/°	90
Volume/$Å^3$	4782.5(3)
Z	4
ρ_{calc}g/cm^3	1.462
μ/mm^{-1}	0.954
F(000)	2160.0
Crystal size/mm^3	0.28 × 0.22 × 0.12
Radiation	MoKα (λ = 0.71073)
2Θ range for data collection/°	2.89 to 53.322
Index ranges	$-14 \leq h \leq 14$, $-35 \leq k \leq 33$, $-19 \leq l \leq 16$
Reflections collected	34839
Independent reflections	10079 [R_{int} = 0.1020, R_{sigma} = 0.1504]
Data/restraints/parameters	10079/3/654
Goodness-of-fit on F^2	0.934
Final R indexes [I>=2σ (I)]	R_1 = 0.0575, wR_2 = 0.0980
Final R indexes [all data]	R_1 = 0.1352, wR_2 = 0.1083
Largest diff. peak/hole / e $Å^{-3}$	1.11/-0.46